# REPORT No. 834

## EFFECT OF COMPRESSIBILITY AT HIGH SUBSONIC VELOCITIES ON THE LIFTING FORCE ACTING ON AN ELLIPTIC CYLINDER

By Carl Kaplan


### SUMMARY

*An extended form of the Ackeret iteration method, applicable to arbitrary profiles, is utilized to calculate the compressible flow at high subsonic velocities past an elliptic cylinder. The angle of attack to the direction of the undisturbed stream is small and the circulation is fixed by the Kutta condition at the trailing end of the major axis. The expression for the lifting force on the elliptic cylinder is derived and shows a first-step improvement of the Prandtl-Glauert rule. It is further shown that the expression for the lifting force, although derived specifically for an elliptic cylinder, may be extended to arbitrary symmetrical profiles.*


### INTRODUCTION

Two methods of approximation, complementary in nature, have been used for the solution of problems of flow past bodies in the subsonic-velocity range. They are the Janzen-Rayleigh method (reference 1), in which the velocity potential or the stream function is developed in a power series of the stream Mach number, and the Ackeret iteration method (reference 2), in which the velocity potential or the stream function is developed in a power series of a geometrical parameter characteristic of the body. The complementary nature of these two methods lies in the fact that the Janzen-Rayleigh procedure yields accurate results in the case of thick bodies, for which the critical stream Mach numbers are low; whereas the Ackeret iteration process yields accurate results in the case of slender shapes, for which the critical stream Mach numbers are in the neighborhood of unity.

In the Ackeret iteration process the assumption is made that, if $\lambda$ is a parameter that represents the departure of the profile shape from a straight-line segment at zero angle of attack (that is, $\lambda$ may be the thickness, the camber, or the angle of attack), the stream function $\psi$, say, may be developed in a power series of $\lambda$ in which the coefficients are functions of the plane coordinates $x$ and $y$ and of the stream Mach number $M_1$; that is,

$$\psi=-Uy+f_1(x, y; M_1)\lambda+f_2(x, y; M_1)\lambda^2+\ldots \qquad (1)$$

where $U$ is the velocity of the undisturbed flow. By inserting this expression into the fundamental nonlinear differential equation for $\psi$ and by equating the coefficients of the various powers of $\lambda$ to zero, a system of linear differential equations for the functions $f_n(x,y;M_1)$ is obtained. The integration of this system of differential equations can be performed for as many steps as desired, the first step $f_1(x,y;M_1)$ being equivalent to the Prandtl-Glauert approximation. There is, however, a fundamental difficulty with the form of the development, equation (1), which does not appear in the Janzen-Rayleigh method. In the Janzen-Rayleigh method the expansion of the stream function in powers of the stream Mach number, namely,

$$\psi=\psi_0+\psi_1M_1^2+\psi_2M_1^4+\ldots \qquad (2)$$

can always be obtained, whereas the possibility of the expansion, equation (1), cannot be guaranteed beforehand. This difficulty in the Ackeret process was avoided in references 3 and 4 by choosing as solid boundaries profiles having no stagnation points. In such cases, a development of the form of equation (1) is always possible. When, however, shapes are chosen that possess stagnation points, terms of the type $\lambda^n \log \lambda$ ultimately appear on the right-hand side of equation (1) and the explicit development in powers of $\lambda$ is strictly no longer possible. This difficulty may be avoided by assuming a somewhat more general form for the development of the stream function; namely,

$$\psi=-Uy+\psi_1(x, y)+\psi_2(x, y)+\ldots \qquad (3)$$

where the shape parameter $\lambda$ is contained implicitly in the various functions $\psi_n$. In equation (3) $\psi_1$ corresponds to the Prandtl-Glauert approximation and $\psi$ is made to satisfy the exact boundary conditions at the solid and at infinity. For the purpose of defining and controlling the iteration procedure, the function $\psi_{n+1}$ is regarded as small compared with the preceding function $\psi_n$ and the derivatives have a similar relationship. It can be stated now that the aforementioned difficulty is more apparent than real, for in carrying out the iterative steps according to equation (1) $\lambda$ behaves like a dummy parameter, which serves only to regulate the iteration process in exactly the same manner as equation (3).

For slender bodies the first few steps of the Ackeret iteration method may be expected to yield a good result with the exception of a small region in the neighborhood of a stagnation point. Hantzsche, in reference 5, treated the case of an elliptic cylinder at zero incidence in a uniform stream according to Ackeret's process as represented by equation (1), with the exact boundary conditions at the solid and at infinity being satisfied. These calculations were carried through the $\lambda^3$-terms and included a term $\lambda^4 \log \lambda$. A comparison, made in reference 5, of this result with that obtained by the present author according to the Janzen-Rayleigh method

showed agreement in the terms common to the two developments. A similar comparison made for the "bump" in reference 3 also showed complete agreement in the terms common to the two methods. These comparisons illustrate the fact that solutions obtained by the Janzen-Rayleigh and the Ackeret methods are simply different representations of a single unique solution. In particular, it is evident that the Janzen-Rayleigh method, which is valid at stagnation points, includes parts of the Ackeret development and, conversely, the Ackeret development includes parts of the Janzen-Rayleigh result. Although the first few terms of equation (3) do not yield very accurate results at stagnation points, these terms nevertheless represent correctly, to some extent, the effect of compressibility at such points. The accuracy of the calculations obviously depends on the number of terms $\psi_n$ derived, each new term reducing the extent of the region of inaccuracy in the neighborhood of a stagnation point.

The question of the convergence of the sequence of functions, equation (3), is a difficult one and should be thoroughly investigated. Schmieden and Kawalki (reference 6) state that both the Janzen-Rayleigh and the Ackeret developments diverge when the local velocity of sound is first exceeded in the region of flow, that is, at the critical value of the stream Mach number. This statement is contradicted, however, by results obtained by means of hodograph or velocity variables. In general, as shown in reference 7, the limit of steady potential flow of a compressible fluid is determined by the vanishing of the Jacobian of the transformation from physical $x$, $y$-variables to hodograph $\theta$, $q$-variables. The vanishing of this functional determinant does not necessarily occur when the local Mach number first reaches unity and, consequently, there exist continuous solutions of the general differential equation governing the flow of a compressible fluid for which a part of the region of flow is supersonic. It is reasonable to conclude, therefore, that the series solutions given by equations (2) and (3) diverge at the value of the stream Mach number that marks the limit of potential flow rather than at the value for which the local velocity of sound is first exceeded in the flow.

The Ackeret process in the form of equation (1), but for the velocity potential, was used to calculate the flow past a bump and past a circular arc profile in references 3 and 4, respectively. This calculation was possible because the profiles considered did not possess stagnation points. As a consequence, the problem could be treated completely in the physical plane and, moreover, the boundary conditions on the velocity potential were tractable. In general, however, when shapes with stagnation points are treated, the Ackeret process in the form of equation (3) instead of in the form of equation (1) should be utilized. In such cases the problem is most conveniently treated in a new plane related to the plane of flow by an affine transformation. In this plane, however, the boundary conditions for the velocity potential become very complicated. On the other hand, the boundary condition for the stream function, $\psi=0$ at the solid, is invariant for affine transformations and it is therefore suggested that the stream function be utilized. The transference of the problem to an affinely connected plane unfortunately introduces a distortion in the actual profile that varies with the stream Mach number. In the case of an elliptic profile, however, this distortion does not matter, for the affine distortion of an ellipse leads to another ellipse. This property of the ellipse makes it a preferred profile for the Ackeret iteration process in the form of equation (3) and is also the reason it is chosen as the solid boundary for the problem treated in the present paper. Specifically, the problem treated herein is the determination of the flow of a compressible fluid past an elliptic cylinder set at a small angle of incidence in a uniform stream, with circulation determined by the Kutta condition at the trailing end of the major axis. The main purpose of this calculation is to obtain some information with regard to the effect of compressibility at high subsonic stream Mach numbers on the lifting force acting on an elliptic cylinder. A calculation is now in progress in the Physical Research Division of the Langley Memorial Aeronautical Laboratory to find the effect of compressibility at high subsonic stream Mach numbers on the moment and on the location of the center of pressure of an elliptic cylinder.

## CALCULATION OF THE FIRST AND SECOND APPROXIMATIONS

The equation of continuity can be written as

$$\frac{\partial}{\partial X}\left(\frac{\rho}{\rho_1}u\right)+\frac{\partial}{\partial Y}\left(\frac{\rho}{\rho_1}v\right)=0 \tag{4}$$

and the condition for irrotational flow as

$$\frac{\partial v}{\partial X}-\frac{\partial u}{\partial Y}=0 \tag{5}$$

where

$X$, $Y$ rectangular Cartesian coordinates in physical flow plane
$u$, $v$ components of velocity along $X$-axis and $Y$-axis, respectively
$\rho$ variable density of fluid
$\rho_1$ constant density of undisturbed fluid at infinity

Equation (5) defines a velocity potential $\phi$, where

$$\left.\begin{aligned} u&=\frac{\partial\phi}{\partial X}\\ v&=\frac{\partial\phi}{\partial Y}\end{aligned}\right\} \tag{6}$$

and equation (4) defines a mass flow or stream function $\psi$, where

$$\left.\begin{aligned} u&=\frac{\partial\phi}{\partial X}=\frac{\rho_1}{\rho}\frac{\partial\psi}{\partial Y}\\ v&=\frac{\partial\phi}{\partial Y}=-\frac{\rho_1}{\rho}\frac{\partial\psi}{\partial X}\end{aligned}\right\} \tag{7}$$

From equations (4) and (5), with the use of equations (6) and (7), respectively, the following alternate forms of the basic differential equation are obtained:

$$\frac{\partial}{\partial X}\left(\frac{\rho}{\rho_1}\frac{\partial\phi}{\partial X}\right)+\frac{\partial}{\partial Y}\left(\frac{\rho}{\rho_1}\frac{\partial\phi}{\partial Y}\right)=0 \tag{8}$$

and

$$\frac{\partial}{\partial X}\left(\frac{\rho_1}{\rho}\frac{\partial\psi}{\partial X}\right)+\frac{\partial}{\partial Y}\left(\frac{\rho_1}{\rho}\frac{\partial\psi}{\partial Y}\right)=0 \tag{9}$$

For reasons stated in the "Introduction," equation (9) for the stream function will be treated in the present paper. The difficulty of obtaining a solution lies in the fact that the density of the fluid $\rho$ is related to $u$ and $v$ because of the dependence of $\rho$ on the local pressure. If it is postulated that the fluid is nonviscous and if the fluid is assumed to flow from infinity with a constant velocity $U$, the total energy of the fluid will then have the same value at every point in the region of flow. If $p$ and $q$ denote the pressure and the velocity of the fluid, respectively, Bernoulli's equation becomes

$$\int_1 \frac{dp}{\rho}+\frac{1}{2}(q^2-U^2)=0 \tag{10}$$

where the lower limit of integration refers to the starting conditions at infinity. Moreover, $p$ and $\rho$ are connected by some known adiabatic equation of state such as

$$\frac{p}{\rho^\gamma}=\frac{p_1}{\rho_1{}^\gamma}=\text{Constant} \tag{11}$$

where, in the case of a perfect gas, $\gamma$ denotes the ratio of specific heats at constant pressure and at constant volume.

By means of the definition of the velocity of sound,

$$c^2=\frac{dp}{d\rho}=\gamma\frac{p}{\rho} \tag{12}$$

the following relations are obtained from equation (10):

$$c^2=c_1{}^2\left[1-\frac{\gamma-1}{2}M_1{}^2\left(\frac{q^2}{U^2}-1\right)\right] \tag{13}$$

$$\rho=\rho_1\left[1-\frac{\gamma-1}{2}M_1{}^2\left(\frac{q^2}{U^2}-1\right)\right]^{\frac{1}{\gamma-1}} \tag{14}$$

$$p=p_1\left[1-\frac{\gamma-1}{2}M_1{}^2\left(\frac{q^2}{U^2}-1\right)\right]^{\frac{\gamma}{\gamma-1}} \tag{15}$$

where $M_1=\frac{U}{c_1}$ is the Mach number of the undisturbed stream at infinity and $q^2=u^2+v^2$.

By means of equations (7), equation (14) can be rewritten in the form

$$\frac{\rho_1}{\rho}=\left\{1-\frac{\gamma-1}{2}M_1{}^2\left[\frac{\rho_1{}^2}{\rho^2}\left(\frac{\psi_X{}^2+\psi_Y{}^2}{U^2}-1\right)+\frac{\rho_1{}^2}{\rho^2}-1\right]\right\}^{-\frac{1}{\gamma-1}} \tag{16}$$

where $\psi_X$ and $\psi_Y$ denote $\partial\psi/\partial X$ and $\partial\psi/\partial Y$, respectively. If, for the moment, $\rho_1/\rho$ and $\frac{\psi_X{}^2+\psi_Y{}^2}{U^2}-1$ are considered to be dependent and independent variables, respectively, a Maclaurin expansion in the neighborhood of the undisturbed stream, where $\frac{\psi_X{}^2+\psi_Y{}^2}{U^2}-1=0$ and $\frac{\rho_1}{\rho}=1$, yields

$$\frac{\rho_1}{\rho}=1+\frac{1}{2}(\mu^2-1)\left(\frac{\psi_X{}^2+\psi_Y{}^2}{U^2}-1\right)$$
$$+\frac{1}{8}(\mu^2-1)^2[(\gamma+4)+(\gamma+1)(\mu^2-1)]\left(\frac{\psi_X{}^2+\psi_Y{}^2}{U^2}-1\right)^2+\cdots \tag{17}$$

where $\mu^2=\frac{1}{1-M_1{}^2}$ and $\mu^2-1=\frac{M_1{}^2}{1-M_1{}^2}$. The form of this development has been chosen to be consistent with the Ackeret iteration process, which is essentially an iteration around an undisturbed stream of zero incidence. Corresponding to equation (3),

$$\psi=-UY+\psi_1+\psi_2+\cdots \tag{18}$$

where $\psi_{n+1}$ is regarded as small compared with $\psi_n$ and the derivatives have a similar relationship. When this expression for $\psi$ is substituted into equation (17) and $\psi_{2Y}$ is noted to be of the same order as $\psi_{1X}{}^2$ or $\psi_{1Y}{}^2$, then inclusive of the second power in the derivatives,

$$\frac{\rho_1}{\rho}=1-(\mu^2-1)\frac{\psi_{1Y}}{U}-(\mu^2-1)\left(\frac{\psi_{2Y}}{U}-\frac{\psi_{1X}{}^2+\psi_{1Y}{}^2}{2U^2}\right)$$
$$+\frac{1}{2}(\mu^2-1)^2[(\gamma+4)+(\gamma+1)(\mu^2-1)]\frac{\psi_{1Y}{}^2}{U}+\cdots \tag{19}$$

When this expression for $\rho_1/\rho$ is substituted into the basic differential equation (9) and terms of equal order of magnitude in the derivatives of $\psi_n$ are equated, the following differential equations for $\psi_1$ and $\psi_2$ are obtained:

$$\psi_{1XX}+\mu^2\psi_{1YY}=0 \tag{20}$$

and

$$\psi_{2XX}+\mu^2\psi_{2YY}=(\mu^2-1)\left\{\frac{\psi_{1Y}}{U}\psi_{1XX}+2\frac{\psi_{1X}}{U}\psi_{1XY}\right.$$
$$\left.+\mu^2[3+(\gamma+1)(\mu^2-1)]\frac{\psi_{1Y}}{U}\psi_{1YY}\right\} \tag{21}$$

These differential equations are most easily solved by first applying the affine transformation

$$\left.\begin{aligned}x&=X\\ y&=\frac{1}{\mu}Y=\sqrt{1-M_1{}^2}\,Y\end{aligned}\right\} \tag{22}$$

Equation (20) then becomes a Laplace equation

$$\psi_{1xx}+\psi_{1yy}=0 \tag{23}$$

and equation (21) becomes a Poisson equation

$$\psi_{2xx}+\psi_{2yy}=(\mu^2-1)\left\{\frac{\psi_{1y}}{\mu U}\psi_{1xx}+2\frac{\psi_{1x}}{\mu U}\psi_{1xy}\right.$$
$$\left.+[3+(\gamma+1)(\mu^2-1)]\frac{\psi_{1y}}{\mu U}\psi_{1yy}\right\} \tag{24}$$

For purposes of calculation a new stream function $\psi^*$ may be conveniently introduced, where

$$\psi=\mu U\psi^* \tag{25}$$

From equations (22) it can be seen that

$$\psi_X=\psi_x=\mu U\psi^*{}_x$$

and

$$\psi_Y=\frac{1}{\mu}\psi_y=U\psi^*{}_y$$

so that the undisturbed flows, at zero angles of incidence, in the physical and affinely distorted planes are identical; that is, $(\psi_Y)_1=(U\psi^*{}_y)_1$. With the introduction of the

stream function $\psi^*$, equations (23) and (24) become

$$\psi^*_{1xx}+\psi^*_{1yy}=0 \tag{26}$$

and

$$\psi^*_{2xx}+\psi^*_{2yy}=(\mu^2-1)\{\psi^*_{1y}\psi^*_{1xx}+2\psi^*_{1x}\psi^*_{1xy}+[3+(\gamma+1)(\mu^2-1)]\psi^*_{1y}\psi^*_{1yy}\}$$

or, with the use of equation (26),

$$\psi^*_{2xx}+\psi^*_{2yy}=(\mu^2-1)\{-[2+(\gamma+1)(\mu^2-1)]\psi^*_{1y}\psi^*_{1xx}+2\psi^*_{1x}\psi^*_{1xy}\} \tag{27}$$

Equations (26) and (27) show that, in order to calculate the various approximations, the incompressible flow past the distorted profile in the $xy$-plane must be known. Thus, if a profile is given in the physical $XY$-plane, it will be necessary to find the conformal transformation to a circle of the distorted profile in the $xy$-plane for each value of the stream Mach number, since the affine distortion of a profile depends on the stream Mach number, as shown by equation (22). In general, then, the problem to be solved is the flow past an arbitrary profile in the affinely distorted $xy$-plane. This procedure in general involves the laborious calculations of the coefficients of conformal transformations to a circle for a number of values of the stream Mach number in such a way that the distorted profiles in the $xy$-plane correspond to the given profile in the physical $XY$-plane. In the case of an ellipse, however, the distorted profile is again an ellipse, and it is therefore a simple matter to transfer the results obtained in the $xy$-plane to the $XY$-plane of the original elliptic profile. In the present paper the elliptic profile is so oriented that its major axis lies along the $X$-axis. The relation between the profiles in the two planes is then given by

$$\left.\begin{aligned}
a&=a'\\
b&=\frac{1}{\mu}b'\\
c^2&=c'^2+\frac{\mu^2-1}{\mu^2}b'^2\\
R&=R'+\frac{1-\mu}{2\mu}b'\\
\tan\alpha&=\frac{1}{\mu}\tan\alpha' \text{ (or, to the first order, } \alpha=\frac{1}{\mu}\alpha')
\end{aligned}\right\} \tag{28}$$

where

$$R=\frac{1}{2}(a+b)$$

$a$ semimajor axis of ellipse in affinely distorted plane
$b$ semiminor axis of ellipse in affinely distorted plane
$c$ semifocal distance of ellipse in affinely distorted plane
$\alpha$ angle of incidence of ellipse in affinely distorted plane

and the prime indicates corresponding values in the physical plane.

The solution of equation (26) is in general the imaginary part of an analytic function $w_1(z)$ where $z=x+iy$. (The asterisk has been dropped.) It is easy then to verify that

$$\psi_{1x}=\frac{1}{2i}(w_{1z}-\overline{w}_{1\bar{z}})$$

$$\psi_{1y}=\frac{1}{2}(w_{1z}+\overline{w}_{1\bar{z}})$$

$$\psi_{1xy}=\frac{1}{2}(w_{1zz}+\overline{w}_{1\bar{z}\bar{z}})$$

$$\psi_{1xx}=-\psi_{1yy}=\frac{1}{2i}(w_{1zz}-\overline{w}_{1\bar{z}\bar{z}})$$

where a bar indicates conjugate-complex quantities. Therefore,

$$2\psi_{1y}\psi_{1xx}=\text{I. P. }(w_{1zz}w_{1z}+w_{1zz}\overline{w}_{1\bar{z}})=(w_{1z}+\overline{w}_{1\bar{z}})\text{ I. P. }w_{1zz}$$

and

$$2\psi_{1x}\psi_{1xy}=\text{I. P. }(w_{1zz}w_{1z}-w_{1zz}\overline{w}_{1\bar{z}})=-i(w_{1z}-\overline{w}_{1\bar{z}})\text{ R. P. }w_{1zz}$$

Equation (27) can then be written as

$$\frac{\partial^2\psi_2}{\partial z\partial\bar{z}}=-\frac{1}{8}(\mu^2-1)\text{ I. P.}\left[\frac{1}{2}\sigma(w_{1z}^2)_z+(\sigma+4)(w_{1z}\overline{w}_{1\bar{z}})_z\right] \tag{29}$$

where $\sigma=(\gamma+1)(\mu^2-1)$.

Consider now a circle of radius $R$, with its center at the origin of the $z'$-plane, into which the distorted profile in the $z$-plane is mapped by means of a conformal transformation. Any point on the circle can be expressed in the form

$$z'=x'+iy'=R(\cos\xi-i\sin\xi)=Re^{-i\xi}$$

so that the point describes the circle in the clockwise sense and leaves the region outside the circle on the left. If now $\zeta=\xi+i\eta$, the transformation

$$z'=Re^{-i\zeta} \tag{30}$$

yields a circle of radius $R$ when $\eta=0$ and the infinite region of the $z'$-plane when $\eta=+\infty$. Equation (30) can be looked upon as the transformation from Cartesian coordinates $x'$, $y'$ to polar coordinates $Re^{\eta}$,$-\xi$. The conformal transformation of an arbitrary profile in the $z$-plane into a circle of radius $R$ in the $z'$-plane, with center at the origin, can therefore be written

$$z=f(e^{i\zeta}) \tag{31}$$

where $\eta=0$ yields the parametric equations of the profile in the $z$-plane.

When $\zeta$ and $\bar{\zeta}$ are introduced as independent variables, equation (29) becomes

$$\frac{\partial^2\psi_2}{\partial\zeta\partial\bar{\zeta}}=-\frac{1}{8}(\mu^2-1)\text{I.P.}\left[\frac{1}{2}\sigma(w_{1z}^2)_\zeta\frac{d\bar{z}}{d\bar{\zeta}}+(\sigma+4)(w_{1z})_\zeta\overline{w}_{1\bar{\zeta}}\right] \tag{32}$$

The general solution of equation (32) or of equation (29) is obtained directly and is

$$\psi_2=-\frac{1}{8}(\mu^2-1)\text{ I.P.}\left[\frac{1}{2}\sigma\bar{z}w_{1z}^2+(\sigma+4)\overline{w}_1w_{1z}+F(\zeta)\right] \tag{33}$$

where $F(\zeta)$ is an arbitrary function to be determined according to the boundary conditions at the solid surface and at infinity.

Consider now an ellipse in the affine $z$-plane with semimajor axis $a$ and semiminor axis $b$. The undisturbed stream at infinity makes a small angle $\alpha$ with the negative direction of the $x$-axis, and the circulation is determined according to the Kutta condition that the downstream end of the major axis is a stagnation point. In accordance with the Ackeret process,

$$\psi=-y+\psi_1+\psi_2+\ldots \tag{34}$$

so that the stream function is expanded around an undisturbed stream at zero incidence. Since the angle of attack has been assumed small, powers of $\alpha$ higher than the first are neglected. The boundary conditions are then, at the surface of the ellipse, $\eta=0$,

$$\left.\begin{aligned}\psi_1&=y\\ \psi_2&=0\end{aligned}\right\} \tag{35a}$$

and, at infinity, $\eta=\infty$,

$$\left.\begin{aligned}\frac{\partial\psi_1}{\partial x}&=-\alpha\\ \frac{\partial\psi_1}{\partial y}&=0\\ \frac{\partial\psi_2}{\partial x}&=0\\ \frac{\partial\psi_2}{\partial y}&=0\end{aligned}\right\} \tag{35b}$$

Now, the transformation

$$z=z'+\frac{c^2}{4z'} \tag{36}$$

maps the region external to the ellipse in the $z$-plane into the region external to a circle of radius $R=\frac{1}{2}(a+b)$ with center at the origin of the $z'$-plane. The complex potential for the flow considered is given by

$$w=-\left(z'e^{i\alpha}+\frac{R^2e^{-i\alpha}}{z'}\right)-2iR\sin\alpha\log\frac{z'}{R} \tag{37}$$

When the variable $\zeta$ is introduced by means of equation (30), equation (36) becomes

$$z=c\cos(\zeta+i\lambda) \tag{38a}$$

and equation (37) becomes

$$w=-2R\cos(\zeta-\alpha)-2R\zeta\sin\alpha \tag{38b}$$

where $a=c\cosh\lambda$ and $b=c\sinh\lambda$. This expression for $w$ includes the uniform undisturbed stream $-z$ which must be extracted in order to obtain $\psi_1$. Thus, for a small angle of attack $\alpha$,

$$w_1=c\cos(\zeta+i\lambda)-2R\cos\zeta-2R(\sin\zeta+\zeta)\alpha \tag{39}$$

and

$$\begin{aligned}\psi_1&=\text{I.P.}w_1\\ &=-c\sinh(\eta+\lambda)\sin\xi+2R\sinh\eta\sin\xi-2R(\sinh\eta\cos\xi+\eta)\alpha\end{aligned}$$

It can be easily verified that this expression for $\psi_1$ satisfies the boundary conditions stated in equations (35) and also that the downstream end of the major axis is a stagnation point.

Similarly, the most direct way to determine $\psi_2$ is to consider it to be the imaginary part of a nonanalytic function $w_2$ of $\zeta$ and $\bar{\zeta}$. Thus, from equations (33), (38), and (39),

$$w_2=-\frac{1}{8}(\mu^2-1)\left\{\frac{1}{2}\sigma c\cos(\bar{\zeta}-i\lambda)w_{1z}^2+(\sigma+4)c[\cos(\bar{\zeta}-i\lambda)-2\frac{R}{c}\cos\bar{\zeta}-2\frac{R}{c}\alpha(\sin\bar{\zeta}+\bar{\zeta})]w_{1z}+F(\zeta)\right\}$$

In order to satisfy the boundary condition $\psi_2=0$ at the surface, $\eta=0$, it is a simple matter to supply the functions of $\zeta$ needed to make the coefficients of $w_{1z}$ and $w_{1z}^2$ vanish for $\eta=0$. For example, $\cos(\bar{\zeta}-i\lambda)=\cos(\zeta-i\lambda)$ for $\eta=0$. Thus,

$$\begin{aligned}\psi_2=-\frac{1}{8}(\mu^2-1)\,\text{I.P.}\Big\{&\frac{1}{2}\sigma c[\cos(\bar{\zeta}-i\lambda)-\cos(\zeta-i\lambda)]w_{1z}^2\\ &+(\sigma+4)c\left[\cos(\bar{\zeta}-i\lambda)-2\frac{R}{c}\cos\bar{\zeta}-2\frac{R}{c}\alpha(\sin\bar{\zeta}+\bar{\zeta})-\cos(\zeta-i\lambda)+2\frac{R}{c}\cos\zeta+2\frac{R}{c}\alpha(\sin\zeta+\zeta)\right]w_{1z}\Big\}\end{aligned} \tag{40}$$

In order to satisfy the boundary condition at infinity and the condition that the downstream end of the major axis be a stagnation point, the procedure, according to equations (7), (22), and (25), is as follows:

$$\frac{\rho}{\rho_1 U}\left(u_2-\frac{i}{\mu}v_2\right)=2i\frac{d\zeta}{dz}\frac{\partial\psi_2}{\partial\zeta}=\frac{d\zeta}{dz}\frac{\partial}{\partial\zeta}(w_2-\bar{w}_2) \tag{41}$$

From equations (39) to (41) it then follows that at infinity

$$\frac{\rho}{\rho_1 U}\left(u_2-\frac{i}{\mu}v_2\right)_{\eta=\infty}=\frac{1}{4}(\mu^2-1)(\sigma+4)\frac{b}{a+b}i\alpha$$

Hence, in order to satisfy the boundary conditions at infinity, $u_2=\frac{\partial\psi_2}{\partial y}=0$ and $v_2=-\frac{\partial\psi_2}{\partial x}=0$, a term $-\frac{1}{4}b\,(\mu^2-1)(\sigma+4)\,\alpha\sin\zeta$, the imaginary part of which vanishes for $\eta=0$, must be added to the expression for $w_2$. This addition to $w_2$ introduces a velocity at the downstream end of the major axis, given by

$$\frac{\rho}{\rho_1 U}\left(u_2-\frac{i}{\mu}v_2\right)_{\xi=\pi,\ \eta=0}=-\frac{1}{4}(\mu^2-1)\,(\sigma+4)\,i\alpha$$

Again, in order to render ($\xi=\pi$, $\eta=0$) a stagnation point, a term $-\frac{1}{4}b\,(\mu^2-1)\,(\sigma+4)\,\alpha\zeta$ satisfying the boundary conditions at the solid and at infinity must be added to the expression for $w_2$. Finally then

$$\begin{aligned}\psi_2&=\text{I. P. } w_2\\&=-\frac{1}{8}(\mu^2-1)\text{ I. P. }\Big\{\frac{1}{2}\sigma c\,[\cos(\bar\zeta-i\lambda)-\cos(\zeta-i\lambda)]\,w_{1z}^2+(\sigma+4)\,c\Big[\cos(\bar\zeta-i\lambda)-2\frac{R}{c}\cos\bar\zeta\\&\quad-2\frac{R}{c}\alpha(\sin\bar\zeta+\bar\zeta)-\cos(\zeta-i\lambda)+2\frac{R}{c}\cos\zeta+2\frac{R}{c}\alpha(\sin\zeta+\zeta)\Big]w_{1z}+2b\,(\sigma+4)(\sin\zeta+\zeta)\,\alpha\Big\}\end{aligned}\tag{42}$$

The complete expression for $\psi$, obtained from equations (34), (39), and (42), is then given by

$$\begin{aligned}\psi=-\text{I. P. }\Big(&2R\cos\zeta+2R\alpha(\sin\zeta+\zeta)+\frac{1}{8}(\mu^2-1)\Big\{\frac{1}{2}\sigma c\,[\cos(\bar\zeta-i\lambda)-\cos(\zeta-i\lambda)]w_{1z}^2\\&+(\sigma+4)c\Big[\cos(\bar\zeta-i\lambda)-2\frac{R}{c}\cos\bar\zeta-2\frac{R}{c}\alpha(\sin\bar\zeta+\bar\zeta)-\cos(\zeta-i\lambda)+2\frac{R}{c}\cos\zeta+2\frac{R}{c}\alpha(\sin\zeta+\zeta)\Big]w_{1z}\\&+2b(\sigma+4)\alpha(\sin\zeta+\zeta)\Big\}\Big)\end{aligned}\tag{43}$$

where $w_1$ is obtained from equation (39) and $w_{1z}=\frac{dw_1}{d\zeta}\frac{d\zeta}{dz}$.

## CALCULATION OF THE VELOCITY COMPONENTS $u$ AND $v$

The components $u$ and $v$ of the velocity of the compressible fluid past the actual profile in the physical $XY$-plane can be put into the following convenient form by means of equations (7), (22), and (25):

$$\frac{\rho}{\rho_1 U}\left(u-\frac{i}{\mu}v\right)=\frac{\partial\psi}{\partial y}+i\frac{\partial\psi}{\partial x}=2i\frac{d\zeta}{dz}\frac{\partial\psi}{\partial\zeta}=\frac{d\zeta}{dz}\frac{\partial}{\partial\zeta}(w-\bar w)\tag{44}$$

where $w$ is the expression on the right-hand side of equation (43) with I. P. omitted. It follows that

$$\begin{aligned}\frac{\rho}{\rho_1 U}\left(u-\frac{i}{\mu}v\right)=\frac{1}{\sin(\zeta+i\lambda)}\Big(&2\frac{R}{c}[-\sin\zeta+\alpha(1+\cos\zeta)]+\frac{1}{4}(\mu^2-1)(\sigma+4)(1+\cos\zeta)\frac{b}{c}\alpha\\&+\frac{1}{8}(\mu^2-1)\,\sigma\Big\{\frac{1}{2}[w_{1z}^2\sin(\zeta-i\lambda)+\bar w_{1\bar z}^2\sin(\zeta+i\lambda)]-[\cos(\zeta-i\lambda)-\cos(\bar\zeta-i\lambda)]w_{1z}w_{1z\zeta}\Big\}\\&+\frac{1}{8}(\mu^2-1)(\sigma+4)\Big\{\Big[\sin(\zeta-i\lambda)-2\frac{R}{c}\sin\zeta+2\frac{R}{c}\alpha(1+\cos\zeta)\Big]w_{1z}+\Big[\sin(\zeta+i\lambda)-2\frac{R}{c}\sin\zeta+2\frac{R}{c}\alpha(1+\cos\zeta)\Big]\bar w_{1\bar z}\\&+\Big[\cos(\bar\zeta-i\lambda)-2\frac{R}{c}\cos\bar\zeta-2\frac{R}{c}\alpha(\sin\bar\zeta+\bar\zeta)-\cos(\zeta-i\lambda)+2\frac{R}{c}\cos\zeta+2\frac{R}{c}\alpha(\sin\zeta+\zeta)\Big]w_{1z\zeta}\Big\}\Big)\end{aligned}\tag{45}$$

where equations (28) provide the correspondence between the distorted ellipse in the $z$-plane and the actual ellipse in the $Z$-plane.

Equation (45) will now be utilized to calculate the lift on an elliptic cylinder in compressible flow. For this calculation a control contour, which eventually is taken as infinitely large, will be applied in the usual manner. The elimination of the variable $\zeta$ in equation (45) and in the equations needed for the calculation of the lift is in general impossible and in the present example undesirable. Since the regions at infinity correspond in the $z$- and $z'$-planes, it is convenient to choose a large circle in the $z'$-plane as the control contour and to effect all the calculations with $\xi$ and $\eta$ as independent variables. The advantage gained by this procedure is a great reduction in labor, in that on a circle $\eta$ is constant and hence only functions of the single variable $z'$ ($=e^{-i\xi}$) appear. The first step is to obtain developments for $\rho u/\rho_1 U$ and $\rho v/\rho_1 U$ in

the neighborhood of infinity and then to form the combination $\frac{\rho}{\rho_1 U}(u-iv)$. This calculation, according to equation (45), yields the following result:

$$\frac{\rho}{\rho_1 U}(u-iv)=-(1+i\mu\alpha)+\frac{i\alpha}{e^{\eta}}\left[1+\frac{1}{4}(\mu^2-1)(\sigma+4)\frac{b}{a+b}\right]\left[(1-\mu)z'-(1+\mu)\frac{1}{z'}\right]$$
$$+\frac{1}{e^{2\eta}}\left\{\left[\frac{b}{a+b}+\frac{1}{4}\left(\frac{b}{a+b}\right)^2(\mu^2-1)(\sigma+4)\right]\left[(1-\mu)z'^2+(1+\mu)\frac{1}{z'^2}\right]+i\alpha\left[\frac{a}{a+b}-\left(\frac{b}{a+b}\right)^2(\mu^2-1)\right]\left[(1-\mu)z'^2-(1+\mu)\frac{1}{z'^2}\right]\right.$$
$$\left.-i\alpha\frac{b}{a+b}(\mu^2-1)\left[\mu\left(z'^2+\frac{1}{z'^2}\right)+(1-\mu)z'^4-(1+\mu)\frac{1}{z'^4}\right]\right\}+\ldots \tag{46}$$

where $z'=e^{-i\xi}$. Since $\frac{\rho u}{\rho_1 U}=\frac{1}{U}\psi_Y$ and $\frac{\rho v}{\rho_1 U}=-\frac{1}{U}\psi_X$, it follows from equations (17) and (46) that

$$\frac{\rho_1}{\rho}=1-\frac{i\alpha}{e^{\eta}}(\mu^2-1)\left[1+\frac{1}{4}(\mu^2-1)(\sigma+4)\frac{b}{a+b}\right]\left(z'-\frac{1}{z'}\right)-\frac{\mu^2-1}{e^{2\eta}}\left\{i\alpha\left[\frac{a}{a+b}-\left(\frac{b}{a+b}\right)^2(\mu^2-1)\right]\left(z'^2-\frac{1}{z'^2}\right)\right.$$
$$\left.+\left[\frac{b}{a+b}+\frac{1}{4}\left(\frac{b}{a+b}\right)^2(\mu^2-1)(\sigma+4)\right]\left[\left(z'^2+\frac{1}{z'^2}\right)+i\alpha\mu^2\left(z'^2-\frac{1}{z'^2}\right)\right]-i\alpha\frac{b}{a+b}(\mu^2-1)\left(z'^4-\frac{1}{z'^4}\right)\right\}+\ldots \tag{47}$$

## CALCULATION OF THE LIFT

In a compressible flow as in an incompressible flow, the lift is given by (reference 8)

$$L_c=\rho_1 U\Gamma_c \tag{48}$$

where $\Gamma_c$ is the circulation round the profile and where, by definition,

$$\Gamma_c=\oint(u\,dX+v\,dY)=\text{R. P.}\oint(u-iv)dZ \tag{49}$$

Now, from equation (22),

$$X=x$$
$$Y=\mu y$$

Hence

$$Z=\frac{1+\mu}{2}z+\frac{1-\mu}{2}z$$

Since $z=c\cos(\zeta+i\lambda)$,

$$dZ=-\frac{1+\mu}{2}c\sin(\zeta+i\lambda)d\zeta-\frac{1-\mu}{2}c\sin(\bar{\zeta}-i\lambda)d\bar{\zeta}$$

For the evaluation of the line integral for $\Gamma_c$, the control contour is a large circle in the $z'$-plane. Therefore, $\eta$ is a constant and $d\zeta=d\bar{\zeta}=i\frac{dz'}{z'}$; hence,

$$dZ=-\frac{ce^{\eta+\lambda}}{4}\left[(1+\mu)\left(\frac{1}{z'e^{2\eta+2\lambda}}-z'\right)+(1-\mu)\left(\frac{1}{z'}-\frac{z'}{e^{2\eta+2\lambda}}\right)\right]\frac{dz'}{z'} \tag{50}$$

where $z'=e^{-i\xi}$. The desired expression for $u-iv$, obtained from equations (46) and (47), is

$$\frac{1}{U}(u-iv)=-1-i\mu\alpha+\frac{i\alpha}{e^{\eta}}\left[1+\frac{1}{4}(\mu^2-1)(\sigma+4)\frac{b}{a+b}\right]\left[(1-\mu)z'-(1+\mu)\frac{1}{z'}+(\mu^2-1)\left(z'-\frac{1}{z'}\right)\right]+\ldots \tag{51}$$

Equations (49) to (51), with only terms containing the factor $dz'/z'$ contributing to the line integral for $\Gamma_c$, then yield the following result:

$$\Gamma_c=4\pi RU\mu^2\alpha\left[1+\frac{1}{8}(\mu^2-1)(\sigma+4)\frac{b}{R}\right] \tag{52}$$

If $a$, $b$, $R$, and $\alpha$ are replaced by $a'$, $b'$, $R'$, and $\alpha'$ according to the correspondence equations (28), then for the actual elliptic cylinder in the physical flow plane $Z$,

$$\Gamma_c=4\pi R'U\alpha'\mu+2\pi U\alpha' b'\left[(1-\mu)+\frac{1}{4}(\mu^2-1)(\sigma+4)\right]$$

Since the circulation in the incompressible case, $M_1=0$ or $\mu=1$, is

$$\Gamma_i=4\pi R'U\alpha'$$

the ratio $\Gamma_c/\Gamma_i$ is given by

$$\frac{\Gamma_c}{\Gamma_i}=\mu+\frac{b'}{2R'}\left[(1-\mu)+\frac{1}{4}(\mu^2-1)(\sigma+4)\right]$$

With $R'=\frac{1}{2}(a'+b')$ and $\sigma=(\gamma+1)(\mu^2-1)$,

$$\frac{L_c}{L_i}=\frac{\Gamma_c}{\Gamma_i}=\mu+\frac{t'}{1+t'}\left[\mu(\mu-1)+\frac{1}{4}(\gamma+1)(\mu^2-1)^2\right] \quad (53)$$

where $t'$ is the thickness coefficient $b'/a'$ of the elliptic cylinder in the physical flow plane. This equation represents a first-step improvement of the Prandtl-Glauert approximation and reduces to that result when $t'\rightarrow 0$.

Although equation (53) has been derived specifically for an elliptic cylinder, it will be shown that the result can be extended to a slender arbitrary symmetrical profile. Hantzsche and Wendt (reference 9) derived a similar relation for the case of a symmetrical Joukowski profile with a sharp trailing edge. The result of Hantzsche and Wendt may be written as

$$\frac{L_c}{L_i}=\frac{\Gamma_c}{\Gamma_i}=\mu+\frac{\epsilon}{1+\epsilon}\left[\mu(\mu-1)+\frac{1}{4}(\gamma+1)(\mu^2-1)^2\right] \quad (54)$$

Note that the function of $\mu$ contained between the brackets is the same in equations (53) and (54). This coincidence suggests a correspondence between the factors $\frac{t'}{1+t'}$ and $\frac{\epsilon}{1+\epsilon}$.

A correspondence is obtained in the following manner: It is well known that by means of the mapping function

$$Z=Z'+\frac{c^2}{4Z'}$$

the circle of radius $c^2/4$, with its center at the origin of the $Z'$-plane, is mapped into the line segment extending from $z=-c$ to $z=c$, and the circle of radius $\frac{c}{2}(1+\epsilon)$, with its center at $Z'=\epsilon\frac{c}{2}$, is mapped into a symmetrical Joukowski profile with sharp trailing edge in the $Z'$-plane. Now

$$\frac{t'}{1+t'}=\frac{R-\frac{c^2}{4R}}{2R} \quad (55)$$

or, with $R=\frac{c}{2}(1+\epsilon)$,

$$\frac{t'}{1+t'}=\frac{1+\epsilon-\frac{1}{1+\epsilon}}{2(1+\epsilon)}$$
$$=\frac{\epsilon}{1+\epsilon}-\frac{1}{2}\left(\frac{\epsilon}{1+\epsilon}\right)^2$$

Thus, to the first power in $\epsilon$, $\frac{t'}{1+t'}=\frac{\epsilon}{1+\epsilon}$ and the correspondence between equations (53) and (54) is established.

In the case of an arbitrary symmetrical profile, the Theodorsen method (see reference 10) is particularly well suited to obtain an expression corresponding to $\frac{t'}{1+t'}$. An essential feature of the potential theory of arbitrary wing profiles developed by Theodorsen is a rapidly convergent procedure for obtaining the conformal transformation of the profile to a circle, also the radius $R$ of the circle. The coefficient of the $\frac{1}{Z'}$-term of this conformal transformation, denoted by $c^2/4$, and the radius $R$ of the conformal circle define an ellipse

$$Z=c\cos(\xi+i\lambda)$$

with

$$R=\frac{c}{2}e^{\lambda}$$

Then, from equation (55),

$$\frac{t'}{1+t'}=\frac{1}{2}(1-e^{-2\lambda})$$

and, therefore, for an arbitrary symmetrical profile, the formula that corresponds to equation (53) may be written

$$\frac{L_c}{L_i}=\frac{\Gamma_c}{\Gamma_i}=\mu+\frac{1}{2}(1-e^{-2\lambda})\left[\mu(\mu-1)+\frac{1}{4}(\gamma+1)(\mu^2-1)^2\right] \quad (56).$$

Table I shows values of the ratio $L_c/L_i$, calculated by means of equation (53), for various values of the thickness coefficient $t'$ and the stream Mach number $M_1$ (with $\gamma=1.4$ for air) and figure 1 shows the corresponding graphs with $M_1$ as abscissa and $L_c/L_i$ as ordinate.

LANGLEY MEMORIAL AERONAUTICAL LABORATORY,
NATIONAL ADVISORY COMMITTEE FOR AERONAUTICS,
LANGLEY FIELD, VA., *May 16, 1946.*

## REFERENCES

1. Rayleigh, Lord: On the Flow of Compressible Fluid past an Obstacle. Phil. Mag., ser. 6, vol. 32, no. 187, July 1916, pp. 1–6.
2. Ackeret, J.: Über Luftkräfte bei sehr grossen Geschwindigkeiten insbesondere bei ebenen Strömungen. Helvetica Physica Acta, vol. I, fasc. 5, 1928, pp. 301–322.

3. Kaplan, Carl: The Flow of a Compressible Fluid past a Curved Surface. NACA Rep. No. 768, 1943.
4. Kaplan, Carl: The Flow of a Compressible Fluid past a Circular Arc Profile. NACA Rep. No. 794, 1944.
5. Hantzsche, W.: Die Prandtl-Glauertsche Näherung als Grundlage für ein Iterationsverfahren zur Berechnung kompressibler Unterschallströmungen. Z.f.a.M.M., Bd. 23, Heft 4, Aug. 1943, pp. 185–199.
6. Schmieden, C., and Kawalki, K. H.: Beiträge zum Umströmungsproblem bei hohen Geschwindigkeiten. Bericht S13/1. Teil der Lilienthal-Gesellschaft für Luftfahrtforschung, 1942, pp. 40–68.
7. Tollmien, W.: Grenzlinien adiabatischer Potentialströmungen. Z.f.a.M.M., Bd. 21, Heft 3, June 1941, pp. 140–152.
8. Theodorsen, Theodore: The Reaction on a Body in a Compressible Fluid. Jour. Aero. Sci., vol. 4, no. 6, April 1937, pp. 239–240.
9. Hantzsche, W., and Wendt, H.: Der Kompressibilitätseinfluss für dünne wenig gekrümmte Profile bei Unterschallgeschwindigkeit. Z.f.a.M.M., Bd. 22, Nr. 2, April 1942, pp. 72–86. (Available as R. T. P. Translation No. 2198, British Ministry of Aircraft Production.)
10. Theodorsen, T., and Garrick, I. E.: General Potential Theory of Arbitrary Wing Sections. NACA Rep. No. 452, 1933.

TABLE I

RATIO OF LIFTS FOR COMPRESSIBLE AND INCOMPRESSIBLE FLOWS

| $M_1$ | $\mu$ | $\mu^2$ | $\frac{\mu^2-\mu}{+0.6(\mu^2-1)^2}$ | $L_c/L_i$ | | | |
|---|---|---|---|---|---|---|---|
| | | | | $t'=0.05$ | $t'=0.10$ | $t'=0.15$ | $t'=0.20$ |
| 0.10 | 1.0050 | 1.0101 | 0.0051 | 1.0053 | 1.0055 | 1.0057 | 1.0059 |
| .20 | 1.0206 | 1.0417 | .0221 | 1.0217 | 1.0226 | 1.0235 | 1.0243 |
| .30 | 1.0483 | 1.0989 | .0565 | 1.0510 | 1.0534 | 1.0557 | 1.0577 |
| .40 | 1.0911 | 1.1905 | .1212 | 1.0969 | 1.1021 | 1.1069 | 1.1113 |
| .45 | 1.1196 | 1.2539 | .1728 | 1.1280 | 1.1355 | 1.1423 | 1.1486 |
| .50 | 1.1547 | 1.3333 | .2453 | 1.1664 | 1.1770 | 1.1867 | 1.1956 |
| .55 | 1.1974 | 1.4337 | .3492 | 1.2140 | 1.2291 | 1.2429 | 1.2556 |
| .60 | 1.2500 | 1.5625 | .5023 | 1.2739 | 1.2957 | 1.3155 | 1.3337 |
| .65 | 1.3159 | 1.7316 | .7376 | 1.3510 | 1.3830 | 1.4121 | 1.4388 |
| .70 | 1.4003 | 1.9608 | 1.1144 | 1.4534 | 1.5016 | 1.5456 | 1.5860 |
| .75 | 1.5119 | 2.2858 | 1.7560 | 1.5955 | 1.6715 | 1.7409 | 1.8046 |
| .80 | 1.6667 | 2.7778 | 3.0074 | 1.8099 | 1.9401 | 2.0589 | 2.1679 |
| .85 | 1.8983 | 3.6037 | 5.7728 | 2.1732 | 2.4231 | 2.6513 | 2.8605 |
| .90 | 2.2942 | 5.2632 | 13.8737 | 2.9548 | 3.5554 | 4.1042 | 4.6064 |

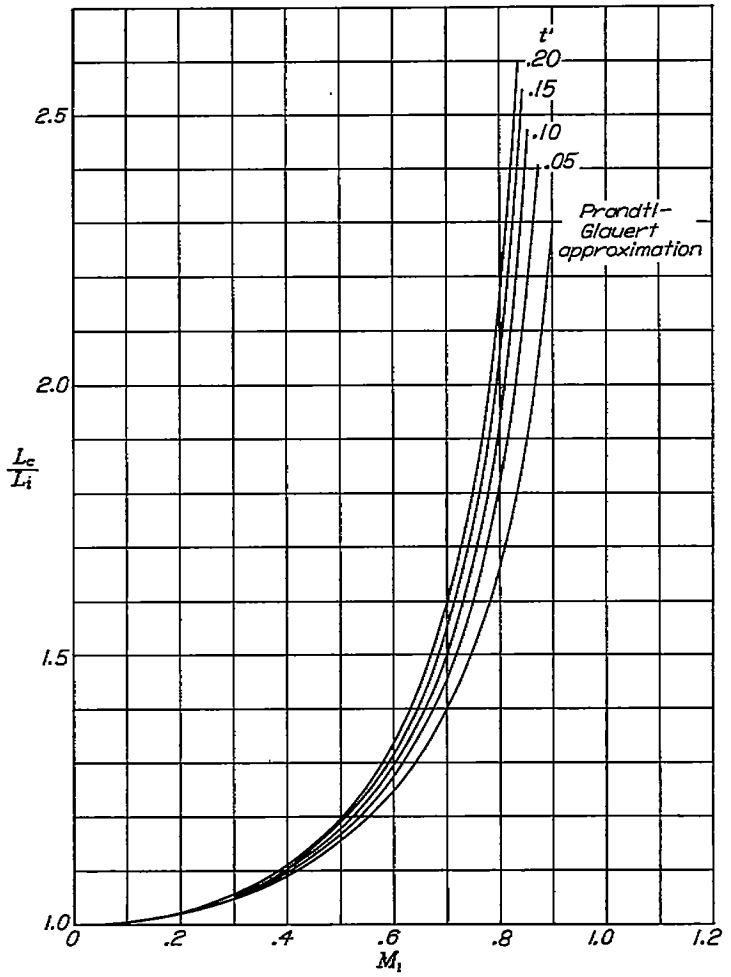


FIGURE 1.—Ratio of lifts for compressible and incompressible fluids as function of stream Mach number.